Carbohydrate Polymers 92 (2013) 523–528

Contents lists available at SciVerse ScienceDirect

Carbohydrate Polymers

journal homepage: www.elsevier.com/locate/carbpol

Synthesis of biocompatible hybrid magnetic hollow spheres based on encapsulation strategy

Wei Ha[a], Hao Wu[a], Yuan Ma[a], Min-Min Fan[b], Shu-Lin Peng[a], Li-Sheng Ding[a], Sheng Zhang[b,*], Bang-Jing Li[a,**]

[a] Chengdu Institute of Biology, Chinese Academy of Sciences, Chengdu 610041, China
[b] State Key Laboratory of Polymer Materials Engineering, Polymer Research Institute of Sichuan University, Sichuan University, Chengdu 610065, China

ARTICLE INFO

Article history:
Received 16 July 2012
Received in revised form 27 August 2012
Accepted 24 September 2012
Available online 2 October 2012

Keywords:
Hollow spheres
Chitosan
Self-assembly
Inclusion chemistry
Magnetofluid
Encapsulation

ABSTRACT

A kind of novel magnetic hollow spheres was prepared by encapsulating magnetofluid into polymeric hollow spheres. Polymeric hollow nanospheres were constructed by self-assembly of rod-coil complexes, in which the rod-like segments were formed by inclusion of α-cyclodextrins (α-CD) and grafting poly(ethylene glycol) (PEG) chains of chitosan-*graft*-PEG (CS-*g*-PEG). Structural characteristics of CS-*g*-PEG/α-CD hollow spheres were investigated in detail by NMR, XRD, TEM, etc. Furthermore, those hollow spheres showed a pH responsive property which induced a considerable change of their radius. Magnetofluid was physically entrapped into the empty domain while hollow spheres were formed, it was found that the hollow spheres can encapsulate large quantities of magnetofluid and the encapsulated magnetofluid still possess magnetic responsiveness properties. We expect that this strategy may be served as a novel and more straightforward approach to obtain magnetic hollow spheres for biomedical application.

1. Introduction

In recent years, the construction of magnetic nanostructures has become a particularly important research field and being attracted growing interest (Arruebo et al., 2006; Nam, Thaxton, & Mirkin, 2003; Yu et al., 2006). Due to their advantages, such as magnetic properties, chemical stability, biocompatibility and low toxicity, magnetic nanocrystals have been intensively studied not only for fundamental scientific interest but also potential applications in biomedical fields, especially in the field of targeted drug delivery (Bráhler et al., 2006; Cao, Zhu, Ma, Li, & Zhang, 2008; Gupta & Gupta, 2005; Hogemann, Ntziachristos, Josephson, & Weissleder, 2002; Hu et al., 2006; Willner & Katz, 2003; Zhao, Kircher, Josephson, & Weissleder, 2002). Pure magnetic nanoparticles are not very useful in practical applications since they are prone to aggregate and rapidly biodegradate when they are directly exposed to a biological system. To overcome these limitations, the magnetic nanoparticles are usually used in the form of core–shell structures or composite nanoparticles (Bruce et al., 2004; Liu, Ma, Xing, & Liu, 2004; Santra et al., 2001). As a kind of ideal material for target drug delivery investigations manipulated by external magnetic fields, nanosized hybrid hollow spheres with magnetic component has attracted much attention owing to their special magnetic properties and great potential for encapsulation of large quantities of guest molecules within the "empty" core domain (Caruso, Spasova, Susha, Giersig, & Caruso, 2001; Pedro, Teresita, & Carlos, 2001; Zhang, Li, Tang, & Ren, 2006).

Currently, the core-template-based strategy is widely used for the synthesis of hybrid magnetic micro or submicron hollow spheres by coating the magnetic components on the polymer particles (Imhof, 2001; Lin, Chen, Wang, & Chen, 2011; Shiho & Kawahashi, 2000; Tissot, Reymond, Lefebvre, & Bourgeat-Lami, 2002; Zhong, Yin, Gates, & Xia, 2000) or layer-by-layer deposition (Caruso, Caruso, & Mohwald, 1998; Caruso et al., 2001; Kawahashi & Matijevic, 1990). One advantage of such an approach is that thickness of the coating layers is controllable. Although it is successful in the preparation of hollow magnetic spheres, core-template-based approach still faces limitations including the selection of core composition and nanosized core templates. Furthermore, the core must be removed to create the hollow center. Hence, a core-template-free strategy for the production of hollow hybrid magnetic hollow spheres is of particular interest (Ding, Hu, Jiang, Zhang, & Yang, 2004; Ding, Hu, Zhang, Chen, & Jiang, 2006; Wong, Cha, Choi, Deming, & Stucky, 2002). However,

* Corresponding author. Tel.: +86 28 85400266; fax: +86 28 85400266/85400266.
** Corresponding author. Tel.: +86 28 85228831/85229227; fax: +86 28 85222384/85223843.
E-mail addresses: zslbj@163.com (S. Zhang), libj@cib.ac.cn (B.-J. Li).

0144-8617/$ – see front matter © 2012 Elsevier Ltd. All rights reserved.
http://dx.doi.org/10.1016/j.carbpol.2012.09.053

recently established core-template-free strategies to prepare hollow hybrid magnetic hollow spheres need harshly physical or chemical procedures which cannot favor to biomedical application.

As well known, hollow spherical aggregates itself have great potentials for encapsulation of large quantities of guest molecules or large sized guests within the "empty" core domain (Bergbreiter, 1999; Cao, Dong, O'Rorke, Wang, & Pandit, 2011; Meier, 2000). Magnetofluid, which has significant superparamagnetism and appropriate size for encapsulation (<10 nm), is a kind of ideal material for constructing magnetic hollow spheres by encapsulation strategy. Therefore, for magnetic target biomedical application, we can try combine delivery and controlled release in one system through filling the hollow core with magnetofluid and desirable drugs. We envision that the strategy of encapsulating magnetofluid into polymer hollow spheres rather than coating magnetic nanoparticles on hollow spheres may be served as a novel and more straightforward approach to obtain magnetic hollow spheres for biomedical application.

In our group, the efforts have been devoted to utilizing rigid/coil system to construct hollow spheres, in which the rod-like blocks are formed by inclusion of the host and guest molecules, the coil-like blocks are always natural polysaccharides and other biocompatible materials. Because of the biocompatible and biodegradable properties, the application of such hollow spheres for enzyme encapsulation and gene delivery was further investigated in detail (Ha et al., 2010, 2011; Li et al., 2011; Meng et al., 2010). In this work presented herein, chitosan (CS) was employed as the matrix of the hollow structure (Wang, Luo, Shao, & Zhou, 2010). We use chitosan-*graft*-PEG (CS-*g*-PEG) as the guest polymer for self-assembly inclusion and the hollow spheres could be formed by inclusion CS-*g*-PEG and α-cyclodextrin (α-CD), in which the rod-like blocks are formed by self-assembly α-CD with poly (ethylene glycol) (PEG). It was found that those hollow spheres showed pH responsive properties which inducing a considerable change of their radius. Furthermore, a kind of much simpler and more straightforward method was applied to construct magnetic hollow spheres, by which entrapping magnetofluid into CS-*g*-PEG/α-CD hollow spheres directly. The obtained magnetic hollow sphere still has magnetic responsiveness and has no effect on the superparamagnetism of magnetofluid which indicates a commendable potential in drug delivery therapeutics.

2. Experimental methods

2.1. Materials and instrument

Chitosan muriate (degree of deacetylation was ≥85%) was purchased from Shandong AK Biotech, Ltd. mPEG (M_W = 2000), 1-ethyl-3-[3-(dimethylamino)propyl]-carbodiamide (EDC), morpholinoethane sulfonic acid (MES) and N-hydroxysuccinimide (NHS) were procured from Sigma–Aldrich (Shanghai, China). α-CD was purchased from TCI Co., Ltd., Tokyo. Hydrophilic magnetofluid was a gift sample obtained from State Key Laboratory of Polymer Materials Engineering, Sichuan University (Chengdu, China). Other reagents were analytical pure and used directly without further purification.

^{1}H NMR was measured on an Avance Bruker-600 spectrometer. The chemical shifts of ^{1}H NMR are expressed in parts per million downfield relative to the internal tetramethylsilane (δ = 0 ppm). IR spectra were recorded on a Perkin Elmer spectrum one FT-IR spectrometer using KBr discs in the range of 400–4000 cm^{-1} region. The crystalline changes in the hollow nanospheres were confirmed by X-ray diffraction measurements, which were performed by using Cu Kα irradiation with PHILP X'Pert MPD (20 kV; 35 mA; 2°/min). The centrifugations were taken on TGL-20M, Saite Centrifuge Co., Shanghai, China. The absorbance value of the solution was recorded on APL-UV-2000 spectrophotometer, Shanghai, China. The TEM observations were performed by JEOL JEM-100CX at an accelerating voltage of 80 kV. The dynamic light scattering (DLS) was measured by BI-9000AT, BI-200SM, Brookhaven Instruments Co., USA.

2.2. Synthesis of CS-g-PEG

2.2.1. Brief procedures

1 g poly(ethylene glycol) methyl ether and 0.5 g NaBr was dissolved in 40 ml water, then 5 ml NaClO and 3 ml TEMPO solution (0.001 mg/ml)were added and a pH was adjusted to 3. The reaction mixture was stirred at ice bath under N_2 for 3 h. Then the reaction solution was extracted three times with chloroform, the organic phases were combined and dried over anhydrous Na_2SO_4. The Na_2SO_4 was filtered, the solvent was evaporated, and the oily residue was dried under vacuum at room temperature to obtain PEG-COOH. **PEG—COOH**: ^{1}H NMR (600 MHz, $CDCl_3$, 25 °C): δ = 3.27 (s; O**CH$_3$**), 4.04 ppm (s; C**H$_2$**COOH), 3.40–3.67 (m; O**CH$_2$CH$_2$**). FT-IR (KBr): 3444 (—OH), 2886 (C—H), 1747 (COOH), 842–1280 (C—O—C) cm^{-1}.

A 5% (w/w) PEG—COOH solution was prepared in a buffer solution of 0.1 M MES and 0.5 M NaCl, and the pH was adjusted to 6. The molar ratio of EDC:NHS:COO^- was 1:0.5:1. A series of sample of NHS and EDC were added to a 2% (w/w) PEG—COOH solution to activate the carboxylic acid groups on the PEG—COOH. The solution was agitated for 10 h to obtain a homogeneous solution followed by the addition of 2% chitosan solution dissolved in MES buffer at pH 4. The solution was dialysed by bag filter (MWCO: 8000–14,000) at 37 °C for 36 h, the solvent was evaporated, washed with acetone 6 times at 60 °C and dried under vacuum at room temperature. **CS-g-PEG**: ^{1}H NMR (600 MHz, D_2O, 25 °C): δ = 3.05 (**H-2** of sugar), 3.24 (s, O**CH$_3$**), 3.43–3.78 (m, O**CH$_2$CH$_2$**), 4.10 (s, **CH$_2$**COOH), 4.75 ppm (**H-1** of sugar). FT-IR (KBr): 3434 (—OH), 2893 (C—H), 1620 (carbonyl), 843–1244 (C—O—C of PEG) cm^{-1}.

2.3. Preparation of self-assembly CS-g-PEG/α-CD hollow spheres

The novel building block of rigid chains of α-CD/PEG was found to be able to self-assemble easily into hollow spheres when PEG-branched chitosan solutions were added dropwise to the α-CD solutions in water. Brief procedures: a series of 1 ml branched chitosan solutions in different degree of PEG substitution were added dropwise into 3 ml α-CD [5% (w/v)] solutions. After stirring for 4 h, the solution turned to muddy and slightly blue, which indicated the formation of hollow spheres. Then the hollow spheres were collected by centrifugation at 16,000 rpm and lyophilized for the further utilization.

2.4. Size distribution of self-assembled hollow spheres

The size and size distribution of CS-*g*-PEG/α-CD self-assembled hollow spheres in water were determined using dynamic laser light-scattering (DLS) with a digital auto correlator at a scattering angle of 90°, a wavelength of 533 nm and a temperature of 25 °C. To investigate the relationship between the degree of PEG substitution and the size of hollow spheres, a series of CS-*g*-PEG/α-CD self-assembled hollow spheres in water with different PEG graft density (DS) of CS-*g*-PEG were prepared. Furthermore, in order to confirm whether the pH value can affect the size of the CS-*g*-PEG/α-CD self-assembled hollow spheres or not, a series of samples with different pH value were prepared.

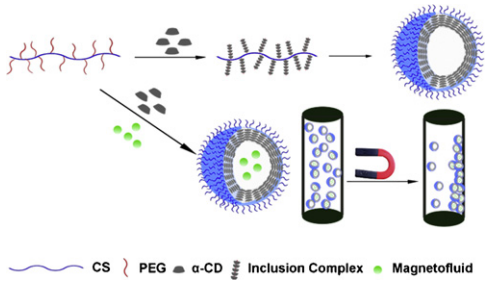

Fig. 1. Schematic illustration of the formation of the CS-*g*-PEG/α-CD hollow sphere and the process of magnetofluid encapsulation.

2.5. Transmission electron microscopy (TEM)

To observe the morphology of CS-*g*-PEG/α-CD self-assembled hollow spheres, sample solutions (0.5 mg/ml) were dropped onto the carbon-coated 300 mesh copper grids. Then, the grids were air-dried and imaged using a transmission electron microscope.

2.6. Preparation of magnetofluid-loaded hollow spheres

1 ml branched chitosan solutions with 0.5 ml magnetofluid solutions were added dropwise into 3 ml α-CD [5%(w/v)] solutions, stirred for 4 h. After the solution turned to muddy, the hollow spheres with entrapped magnetofluid were collected by magnetic separation for further investigation.

3. Results and discussion

3.1. Preparation of CHCKGM conjugates

For the synthesis of CS-*g*-PEG conjugates, mPEG was initially oxidized to carboxylic acid using TEMPO as a catalyst, and then chemically coupled with the primary amino group of CS by using "zero length" crosslinker of EDC/NHS. The DS of PEG moiety could be controlled by the feed ratio of PEG—COOH to CS. The products of CS-*g*-PEG with different DS were characterized by IR spectra and ^{1}H NMR spectra.

Fig. S1 shows the IR spectra of CS (a) and CS-*g*-PEG (b). The absorption band at 1632 cm^{-1} is attributed to the carbonyl of O=C—NHR of chitosan and the absorption band at 1526 cm^{-1} is assigned to the amino groups of chitosan with high deacetylation degrees. This signal shifts to 1465 cm^{-1} after the conjugation reaction, indicating the formation of new amide bonds by acylation of amino groups of chitosan with activated carboxyl groups of PEG—COOH.

The products of CS-*g*-PEG with different DS (degree of substitution) were also confirmed by ^{1}H NMR spectra, as shown in Fig. S2. Compared with the proton signals of CS, the strong —OCH_2 peaks of PEG group are present between 3.5 and 3.8 ppm which prove the presence of PEG in CS conjugates and meanwhile, DS of PEG moiety could be exactly calculated by comparing the ratio of —OCH_3 protons (**b**, peaks in Fig. S2) of PEG to sugar protons (**a**, peaks in Fig. S2). Table 1 summarized the synthetic results of CS-*g*-PEG.

Table 1
Synthetic results of CS-*g*-PEG and the D_h of CS-*g*-PEG self-assembled hollow spheres.

	Feed ratio[a]	DS (%)[b]	D_h (nm)
CS-*g*-PEG1	0.5:1	9.1	1119
CS-*g*-PEG2	1:1	13.8	1076
CS-*g*-PEG3	2:1	16.2	945

[a] The molar ratio of PEG—COOH and sugar unit of CS.
[b] DS of PEG content in CS-*g*-PEG was calculated from the peak integration of ^{1}H NMR spectra.

The resulting CS-*g*-PEGs were water-soluble copolymers, but after this transparent solution was added to α-CD aqueous solution, the mixed solution gradually became turbid. As discussed in our previous work, α-CDs molecules should thread along the PEG chains to form rod-like inclusion blocks and hollow spheres were formed due to the propensity to parallel packing of the rod-like inclusion block grafted on the chitosan chains (Fig. 1). The morphology of the aggregates was studied by transmission electron microscopy (TEM). As shown in Fig. 2(a–c), the obvious contrast between the central and outer part of particles was observed and they were typical TEM images of hollow spheres as reported for different kinds of hollow particles (Chen & Jiang, 2005; Duan, Kuang, Wang, Chen, & Jiang, 2004; Kuang, Duan, Wang, & Jiang, 2004).

The hydrodynamic diameter (D_h) of CS-*g*-PEG/CD in aqueous solution obtained by light scattering is shown in Table 1. The D_h of hollow spheres decreased with the increasing of PEG content in CS-*g*-PEG, which indicated that more grafts favor the formation of smaller aggregates. This tendency of the size varying with "graft density" is quite consistent with that reported for the hydrogen bonding graft complexes in solvent (Chen & Jiang, 2005; Duan & Chen, 2001; Duan et al., 2004; Kuang, Duan, Wang, Chen, & Jiang, 2003; Kuang et al., 2004). In that case, the rod-like rigid polymer "grafting" to the coil-like polymer chains through hydrogen bonding led to the formation of submicron hollow sphere with rod polymer as the inner shell and coil polymer as the outer shell (Kuang et al., 2004).

X-ray diffraction (XRD) results showed the inclusion formation between the CS-*g*-PEG and α-CDs. As shown in Fig. 3, the pattern of CS-*g*-PEG/α-CD particles was similar to that of complex of PEG/α-CD inclusion ($2\theta = 20^\circ$), which has been reported to have a rod channel structure (Harada & Kamachi, 1990; Harada, Li, & Kamachi, 1993; Huang, Allen, & Tonelli, 1998), while the homoPEG crystalline peaks ($2\theta = 19.2^\circ$ and 23.3°) and α-CD crystalline peak ($2\theta = 21.5^\circ$) were absent. This implies that α-CD rings are stacked along the graft PEG chain axis to form a channel-type crystalline structure. As a result, the CS-*g*-PEG/α-CD complexes have both rod block (PEG-α-CD inclusion) and coil block (ionized CS backbone). Jenekhe et al. and Jiang et al. have reported that the rod-like block in rod-coil system preferred parallel packing crowdedly and resulted in the formation of hollow spheres for necessary of the efficient space-filling packing (Chen & Jiang, 2005; Duan & Chen, 2001; Duan et al., 2004; Harada et al., 1993; Huang et al., 1998; Jenekhe & Chen, 1998;

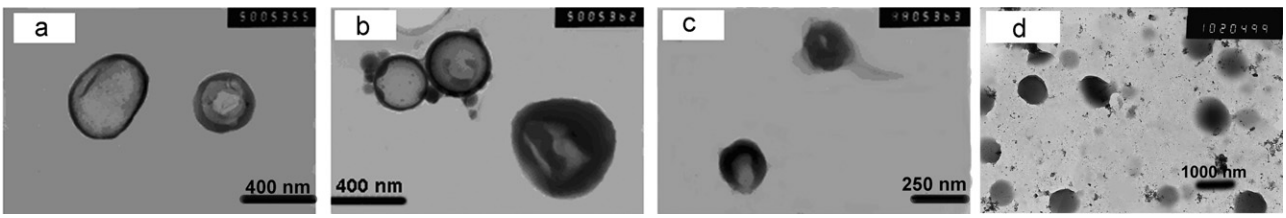

Fig. 2. TEM micrograph of CS-*g*-PEG/α-CD hollow spheres: (a) CS-*g*-PEG1; (b) CS-*g*-PEG2; (c) CS-*g*-PEG3; (d) CS-*g*-PEG2/α-CD hollow nanospheres entrapped with magnetofluid.

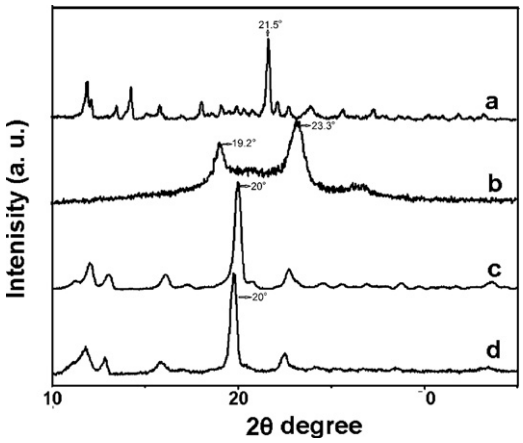

Fig. 3. X-ray diffraction patterns of (a) α-CD; (b) CS-*g*-PEG; (c) complete PEG-α-CD inclusion complex; (d) CS-*g*-PEG/α-CD particles.

Jenekhe & Chen, 1999; Kuang et al., 2003, 2004) With the formation of insoluble PEG-α-CD inclusion blocks, water became a selective solvent for the CS-*g*-PEG/α-CD, so hollow spheres were formed. The expected structure of such an aggregate in aqueous solution is an inner PEG-α-CD inclusion block surrounded by the protonated coil-like CS shell.

The hollow spheres are sensitive nanoparticles toward the physicochemical conditions of their surrounding medium (e.g., ionic strength, pH, or presence of multivalent ions). As shown in Fig. 4, while adjusting the pH value from 6.0 to 2.0, it can be seen that the particles radius decreases from 930 nm to 580 nm, which indicates that those self-aggregated hollow spheres possess pH-dependent properties causing a considerable change of their radius. It is well known that the chitosan chains changed from less soluble hypercoil chains to soluble extended chains as the pH value decreased. At high pH region (pH > 7.0), the chitosan chains were poor soluble because of the protonation of amino groups. Therefore, the CS-*g*-mPEG/α-CD complexes were not stable and macrocosmic precipitation took place. As pH value decreased, the amino group ionizated and then the CS-*g*-mPEG/α-CD complexes became more and more stable.

To further construct the magnetic hollow spheres, magnetofluid was physically entrapped into the empty domain while hollow spheres were formed (Fig. 1). Respectively added CS-*g*-PEG solution with or without magnetofluid dropwise to the solution in water, both mixed solution became turbid gradually. The morphology of the aggregates entrapped with magnetofluid was studied by TEM. As shown in Fig. 2d, there are no bright domains can be found within

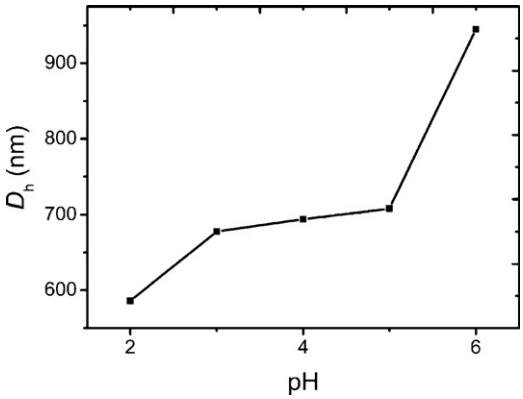

Fig. 4. Average hydrodynamic diameter ⟨D_h⟩ of CS-*g*-PEG1 self-assembled hollow spheres as a function of pH.

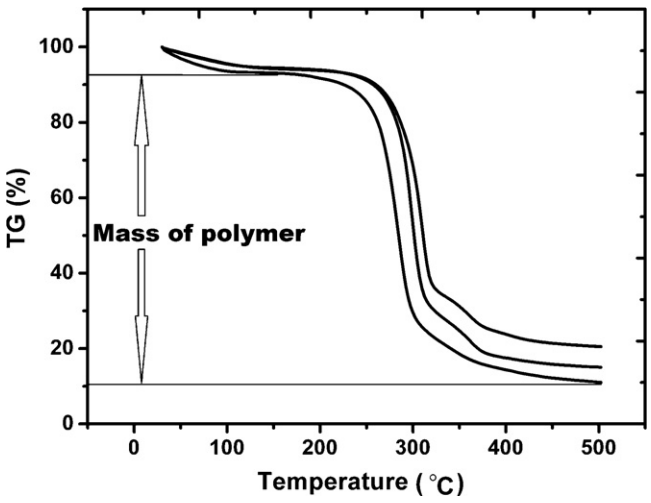

Fig. 5. TGA thermograms of CS-*g*-mPEG2/α-CD hollow spheres entrapped with magnetofluid.

the spheres entrapping magnetofluid. In contrast, the cores of hollow spheres show a little darker than the outlines of spheres and this suggests that the presence of magnetofluid have no effect to the self-assembly procedure and the hollow spheres are filled with magnetofluid.

The encapsulation efficiency of magnetofluid was calculated from TGA results, as shown in Fig. 5, TGA yields an organic weight fraction of CS-*g*-mPEG2/α-CD hollow spheres entrapped with magnetofluid, therefore, the magnetofluid weight fraction in CS-*g*-mPEG2/α-CD magnetic hollow spheres was obtained accordingly. The average values in Fig. 5 were calculated from three-repeated measurements and the encapsulation efficiency of magnetofluid was achieved as 16.6 ± 5.0%.

The paramagnetic properties of CS-*g*-mPEG/α-CD magnetic hollow spheres were measured by vibrating sample magnetometry (VSM) at room temperature and separated from solution under magnetic field. As shown in Fig. 6, the coercive force is close to zero, which means the encapsulation has no effect on the superparamagnetism of magnetofluid and the low magnetic interaction between the hollow spheres and the well dispersibility in solution without magnetic field. Fig. 7 demonstrates the effect of a permanent magnet on both hollow nanospheres and

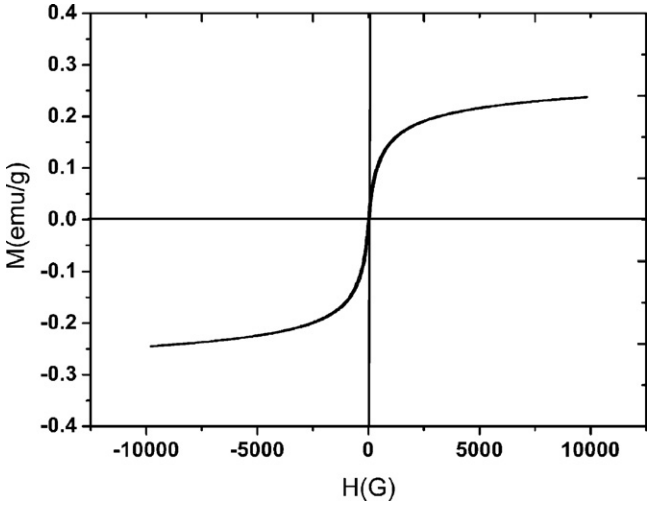

Fig. 6. Room temperature magnetic hysteresis loops of CS-*g*-PEG2/α-CD hollow nanospheres entrapped with magnetofluid.

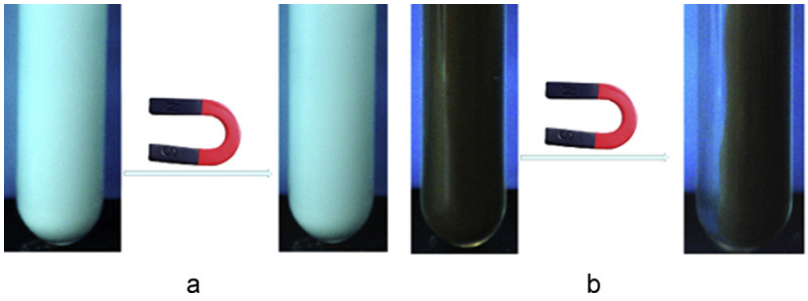

Fig. 7. Pictures of CS-*g*-PEG2/α-CD hollow nanospheres under the effect of a permanent magnet: (a) without magnetofluid; (b) entrapped with magnetofluid.

CS-*g*-PEG/α-CD/magnetofluid particles, as shown in Fig. 7a, there were no effect on the hollow spheres when the magnet is in close to the solutions, however, when the magnetofluid was introduced into the system, as shown in Fig. 7b, most hollow spheres which entrapped with magnetofluid are concentrated at the right-hand side of the bottle when the magnet is placed at the corresponding positions. It is worth noting that the magnetic hollow spheres were attracted toward the magnet above 2 h, which is slower than that of bulk magnetofluid (within 20 s). This result further indicated that magnetofluid was encapsulated into hollow spheres successfully and when the magnetofluid was encapsulated into hollow spheres, the movability response to magnetic field was restricted because the encapsulated magnetofluid must drive the hollow spheres toward the magnet. This phenomenon is consistent with the magnetic hysteresis loop result. As shown in Fig. 6, the saturation magnetization value of the magnetic hollow spheres is 0.23 emu/g, which represents the weak magnetic response to an external magnetic field. The loss of magnetization can be attributed to the encapsulation of magnetofluid. Contrast to most systems for constructing magnetic delivery carrier, the method reported in this paper, by which using CS-*g*-PEG/α-CD hollow spheres for encapsulating magnetofluid directly, seems much simpler and more straightforward. When the permanent magnet is removed, the CS-*g*-PEG/α-CD hollow spheres entrapped with magnetofluid can be re-dispersed well in water again. This is an important characteristic that allows the tracking of such particles in a magnetic gradient without losing the advantage of a stable colloidal suspension and is especially valuable in the field of targeted drug delivery.

4. Conclusion

In conclusion, we presented a convenient approach to construct magnetic hollow spheres through encapsulating magnetofluid into a kind of biocompatible and biodegradable hollow spheres. The strategy of fabricating hollow spheres based on the self-assembly of rod-coil complexes, in which the rod-like segments were formed by supramolecular inclusion. Those self-aggregated hollow spheres showed pH-dependent properties. This pH-switchable control of the polyelectrolyte envelopes can be used to trigger the release of encapsulated drugs. It was found that the encapsualation process has no effect on the superparamagnetism of magnetofluid and the encapsulated magnetofluid still possess magnetic responsiveness properties. We suggest that the encapsulation for magnetofluid presented in this paper represents a new approach to construct magnetic carrier for medical purposes, this concept will enable expanding applications to construct other types of magnetic hollow spheres. Our envision is that these magnetic hollow spheres are very promising for application in targeted drug delivery in the future.

Acknowledgements

This work was funded by the National Natural Science Foundation of China (Grant nos. 21074138 and 51073107), West Light Foundation of CAS, CAS Knowledge Innovation Program (Grant no. KSCX2-EW-J-22) and the Opening Project of State Key Laboratory of Polymer Materials Engineering (Sichuan University) (Grant no. KF201003).

Appendix A. Supplementary data

Supplementary data associated with this article can be found, in the online version, at http://dx.doi.org/10.1016/j.carbpol.2012.09.053.

References

Arruebo, M., Galán, M., Navascués, N., Téllez, C., Marquina, C., Ibarra, M. R., et al. (2006). Development of magnetic nanostructured silica-based materials as potential vectors for drug-delivery applications. *Chemistry of Materials*, *18*, 1911–1919.

Bergbreiter, D. E. (1999). Self-assembled, sub-micrometer diameter semipermeable capsules. *Angewandte Chemie International Edition*, *38*, 2870–2872.

Bráhler, M., Georgieva, R., Buske, N., Müller, A., Müller, S., Pinkernelle, J., et al. (2006). Magnetite-loaded carrier erythrocytes as contrast agents for magnetic resonance imaging. *Nano Letters*, *6*, 2505–2509.

Bruce, I. J., Taylor, J., Todd, M., Davies, M. J., Borioni, E., Sangregorio, C., et al. (2004). Synthesis, characterisation and application of silica-magnetite nanocomposites. *Journal of Magnetism and Magnetic Materials*, *284*, 145–160.

Cao, H. L., Dong, Y. X., O'Rorke, S., Wang, W. X., & Pandit, A. (2011). PEG based hyperbranched polymeric hollow nanospheres. *Nanotechnology*, *22*, 065604.

Cao, S. W., Zhu, Y. J., Ma, M. Y., Li, L., & Zhang, L. (2008). Hierarchically nanostructured magnetic hollow spheres of Fe_3O_4 and γ-Fe_2O_3: Preparation and potential application in drug delivery. *The Journal of Physical Chemistry C*, *112*, 1851–1856.

Caruso, F., Caruso, R. A., & Mohwald, H. (1998). Nanoengineering of inorganic and hybrid hollow spheres by colloidal templating. *Science*, *282*, 1111–1114.

Caruso, F., Spasova, M., Susha, A., Giersig, M., & Caruso, R. A. (2001). Magnetic nanocomposite particles and hollow spheres constructed by a sequential layering approach. *Chemistry of Materials*, *13*, 109–116.

Chen, D. Y., & Jiang, M. (2005). Strategies for constructing polymeric micelles and hollow spheres in solution via specific intermolecular interactions. *Accounts of Chemical Research*, *38*, 494–502.

Ding, Y., Hu, Y., Jiang, X. Q., Zhang, L. Y., & Yang, C. Z. (2004). Polymer–monomer pairs as a reaction system for the synthesis of magnetic Fe_3O_4–polymer hybrid hollow nanospheres. *Angewandte Chemie International Edition*, *43*, 6369–6372.

Ding, Y., Hu, Y., Zhang, L. Y., Chen, Y., & Jiang, X. Q. (2006). Synthesis and magnetic properties of biocompatible hybrid hollow spheres. *Biomacromolecules*, *7*, 1766–1772.

Duan, H. W., & Chen, D. Y. (2001). Self-assembly of unlike homopolymers into hollow spheres in nonselective solvent. *Journal of the American Chemical Society*, *123*, 12097–12098.

Duan, H. W., Kuang, M., Wang, J., Chen, D. Y., & Jiang, M. (2004). Self-assembly of rigid and coil polymers into hollow spheres in their common solvent. *The Journal of Physical Chemistry B*, *108*, 550–555.

Gupta, A. K., & Gupta, M. (2005). Cytotoxicity suppression and cellular uptake enhancement of surface modified magnetic nanoparticles. *Biomaterials*, *26*, 1565–1573.

Ha, W., Meng, X. W., Li, Q., Fan, M. M., Peng, S. L., Ding, L. S., et al. (2010). Self-assembly hollow nanosphere for enzyme encapsulation. *Soft Matter*, *6*, 1405–1408.

Ha, W., Meng, X. W., Li, Q., Fan, M. M., Peng, S. L., Ding, L. S., et al. (2011). Encapsulation studies and selective membrane permeability properties of self-assembly hollow nanospheres. *Soft Matter*, *7*, 1018–1024.

Harada, A., & Kamachi, M. (1990). Complex formation between poly (ethylene glycol) and α-cyclodextrin. *Macromolecules*, *23*, 2821–2823.
Harada, A., Li, J., & Kamachi, M. (1993). Preparation and properties of inclusion complexes of polyethylene glycol with α-cyclodextrin. *Macromolecules*, *26*, 5698–5703.
Hogemann, D., Ntziachristos, V., Josephson, L., & Weissleder, R. (2002). High throughput magnetic resonance imaging for evaluating targeted nanoparticle probes. *Bioconjugate Chemistry*, *13*, 116–121.
Hu, F., Wei, L., Zhou, Z., Ran, Y. L., Li, Z., & Gao, M. Y. (2006). Preparation of biocompatible magnetite nanocrystals for in vivo magnetic resonance detection of cancer. *Advanced Materials*, *18*, 2553–2556.
Huang, L., Allen, E., & Tonelli, A. E. (1998). Study of the inclusion compounds formed between α-cyclodextrin and high molecular weight poly(ethylene oxide) and poly(ε-caprolactone). *Polymer*, *39*, 4857–4865.
Imhof, A. (2001). Preparation and characterization of titania-coated polystyrene spheres and hollow titania shells. *Langmuir*, *17*, 3579–3585.
Jenekhe, S. A., & Chen, X. L. (1998). Self-assembled aggregates of rod-coil block copolymers and their solubilization and encapsulation of fullerenes. *Science*, *279*, 1903–1907.
Jenekhe, S. A., & Chen, X. L. (1999). Self-assembly of ordered microporous materials from rod-coil block copolymers. *Science*, *283*, 372–375.
Kawahashi, N., & Matijevic, E. (1990). Preparation and properties of uniform coated colloidal particles. V. Yttrium basic carbonate on polystyrene latex. *Journal of Colloid and Interface Science*, *138*, 534–542.
Kuang, M., Duan, H. W., Wang, J., Chen, D. Y., & Jiang, M. (2003). A novel approach to polymeric hollow nanospheres with stabilized structure. *Chemical Communications*, 496–497.
Kuang, M., Duan, H. W., Wang, J., & Jiang, M. (2004). Structural factors of rigid-coil polymer pairs influencing their self-assembly in common solvent. *The Journal of Physical Chemistry B*, *108*, 16023–16029.
Li, Q., Xia, B., Ha, W., Wu, H., Meng, X. W., Peng, S. L., et al. (2011). Self-assembly of carboxymethyl konjac glucomannan-*g*-poly(ethylene glycol) and (α-cyclodextrin) to biocompatible hollow nanospheres for glucose oxidase encapsulation. *Carbohydrate Polymers*, *86*, 120–126.
Lin, C. R., Chen, I.-H., Wang, C. C., & Chen, M. L. (2011). Synthesis and characterization of magnetic hollow nanocomposite spheres. *Acta Materialia*, *59*, 6710–6716.
Liu, X., Ma, Z., Xing, J., & Liu, H. (2004). Preparation and characterization of amino-silane modified superparamagnetic silica nanospheres. *Journal of Magnetism and Magnetic Materials*, *270*, 1–6.
Meier, W. (2000). Polymer nanocapsules. *Chemical Society Reviews*, *29*, 295–303.
Meng, X. W., Qin, J., Liu, Y., Fan, M. M., Li, B. J., Zhang, S., et al. (2010). Degradable hollow spheres based on self-assembly inclusion. *Chemical Communications*, *46*, 643–645.
Nam, J. M., Thaxton, C. S., & Mirkin, C. A. (2003). Nanoparticle-based bio-bar codes for the ultrasensitive detection of proteins. *Science*, *301*, 1884–1886.
Pedro, T., Teresita, G. C., & Carlos, J. S. (2001). Coated maghemite hollow spheres with tunable magnetic properties. *Advanced Materials*, *13*, 1620–1624.
Santra, S., Tapec, R., Theodoropoulou, N., Dobson, J., Hebard, A., & Tan, W. H. (2001). Synthesis and characterization of silica-coated iron oxide nanoparticles in microemulsion: The effect of nonionic surfactants. *Langmuir*, *17*, 2900–2906.
Shiho, H., & Kawahashi, N. (2000). Titanium compounds as coatings on polystyrene latices and as hollow spheres. *Colloid & Polymer Science*, *278*, 270–274.
Tissot, I., Reymond, J. P., Lefebvre, F., & Bourgeat-Lami, E. (2002). SiOH-functionalized polystyrene latexes. A step toward the synthesis of hollow silica nanoparticles. *Chemistry of Materials*, *14*, 1325–1331.
Wang, W. J., Luo, C., Shao, S. J., & Zhou, S. B. (2010). Chitosan hollow nanospheres fabricated from biodegradable poly-D,L-lactide–poly(ethylene glycol) nanoparticle templates. *European Journal of Pharmaceutics and Biopharmaceutics*, *76*, 376–383.
Willner, I., & Katz, E. (2003). Magnetische Kontrolle elektrokatalytischer und bioelektrokatalytischer Prozesse. *Angewandte Chemie*, *115*, 4724–4737.
Wong, M. S., Cha, J. N., Choi, K. S., Deming, T. J., & Stucky, G. D. (2002). Assembly of nanoparticles into hollow spheres using block copolypeptides. *Nano Letters*, *2*, 583–587.
Yu, D. B., Sun, X. Q., Zou, J. W., Wang, Z. R., Wang, F., & Tang, K. (2006). A general route to nonspherical anatase TiO_2 hollow colloids and magnetic multifunctional particles. *The Journal of Physical Chemistry B*, *110*, 21667–21671.
Zhang, Y. Q., Li, L. L., Tang, F. Q., & Ren, J. (2006). Controlled drug delivery system based on magnetic hollow spheres/polyelectrolyte multilayer coreshell structure. *Journal of Nanoscience and Nanotechnology*, *6*, 3210–3214.
Zhao, M., Kircher, M. F., Josephson, L., & Weissleder, R. (2002). Differential conjugation of tat peptide to superparamagnetic nanoparticles and its effect on cellular uptake. *Bioconjugate Chemistry*, *13*, 840–844.
Zhong, Z. Z., Yin, Y. D., Gates, B., & Xia, Y. (2000). Preparation of mesoscale hollow spheres of TiO_2 and SnO_2 by templating against crystalline arrays of polystyrene beads. *Advanced Materials*, *12*, 206–209.